Electronic Supplementary Information (ESI)

Stability of polycyclic aromatic hydrocarbons on graphite: Resistance to horizontal displacement

Yoshihiro Kikkawa [a, *] and Seiji Tsuzuki [b, *]

[a] *National Institute of Advanced Industrial Science and Technology (AIST), Tsukuba Central 5, 1-1-1 Higashi, Tsukuba, Ibaraki 305-8565, Japan*

[b] *Department of Applied Physics, The University of Tokyo, Tokyo 113-8656, Japan*

1. Optimised geometry of pyrene-benzene complex

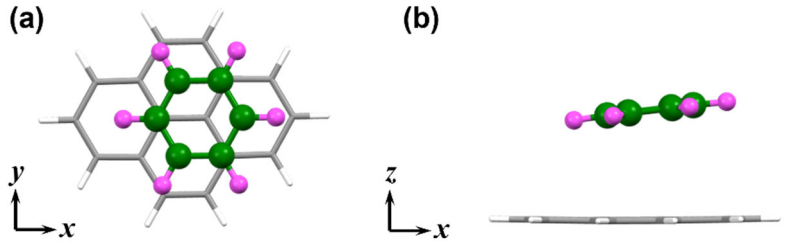

Fig. S1 Optimised geometry of pyrene-benzene complex at B3LYP-D3/6-31G* level, viewed from different directions.

2. Interaction energy potentials of flat-on and edge-on $C_{96}H_{24}$-benzene complex

Interaction energy (E_{int}) potentials were calculated for the $C_{96}H_{24}$-benzene complex at the B3LYP-D3/6-311G** level. The position dependence of the E_{int} for the flat-on (benzene plane is parallel to the plane of $C_{96}H_{24}$) and edge-on (benzene plane is perpendicular to the plane of $C_{96}H_{24}$) $C_{96}H_{24}$-benzene complex was evaluated by calculating E_{int} for a few configurations with changing the distance between $C_{96}H_{24}$ and benzene (R). The positions of flat-on and edge-on benzene are shown in Figs. S2(a-d) and S2(e-h), respectively. In the case of flat-on benzene (Fig. S2(a-d)), equilibrium distance was R = 3.4 Å, whereas that for edge-on benzene was R = 3.5 Å. The E_{int} values for flat-on benzene complexes at the equilibrium distance are larger (more negative) than those for edge-on complexes in all configurations. This is due to the difference in the number of carbon atoms of benzene which are close to underlying $C_{96}H_{24}$. Among the flat-on oriented benzene, configuration (a) (AB stacking) has the largest interaction energy at the equilibrium distance among the four configurations, although the differences in E_{int} between configurations (a) and (b) is small. When the centre of benzene is overlapped with one of six membered ring of $C_{96}H_{24}$ (configurations (c) and (d)), the E_{int} at the equilibrium distance are smaller than that in (a).

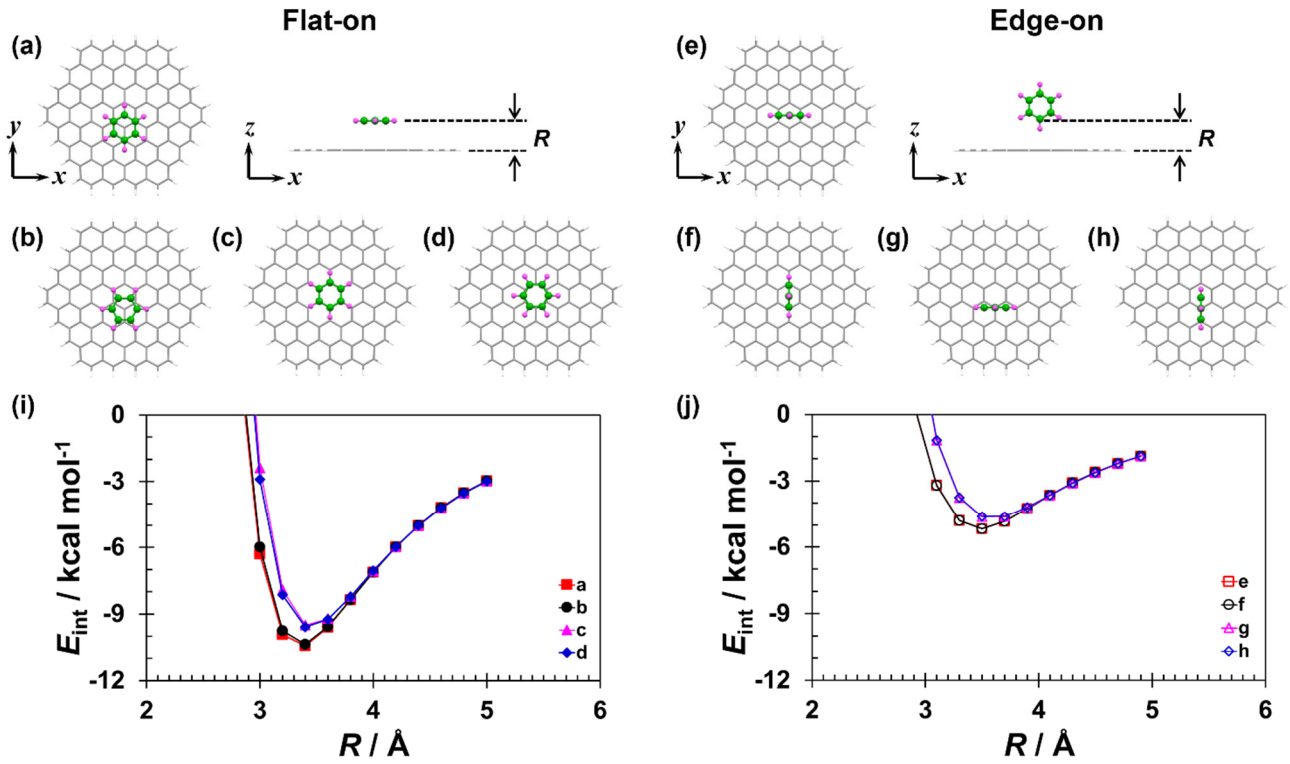

Fig. S2 Geometries of flat-on and edge-on $C_{96}H_{24}$-benzene complex and their interaction energies (E_{int}); (a-d) Configurations of flat-on $C_{96}H_{24}$-benzene complex; (e-h) Configurations of edge-on $C_{96}H_{24}$-benzene complex; (i) B3LYP-D3/6-311G** level E_{int} calculated for flat-on $C_{96}H_{24}$-benzene complexes with changing intermolecular distance (R); (j) B3LYP-D3/6-311G** level E_{int} calculated for edge-on $C_{96}H_{24}$-benzene complexes.

3. Interlayer cohesion energies by previous experiments and theoretical calculations

Table S1 Graphite interlayer cohesion energy determined by experimental methods and theoretical calculations

	Method	Energy / kcal mol^{-1}
Experimental data		
L. X. Benedict *et al.* 1998 [S1]	TEM [a]	$0.81^{+0.35}_{-0.23}$
R. Zacharia *et al.* 2004 [S2]	TPD [b]	1.20 ± 0.10
E. Koren *et al.* 2015 [S3]	AFM [c]	0.86 ± 0.02
J. Wang *et al.* 2016 [S4]	STM[d]	0.84 ± 0.04
J. Weippert *et al.* 2018 [S5]	TPD [b]	1.01 ± 0.09
Theoretical calculation data		
S. D. Chakarova-Käck *et al.* 2006 [S6]	vdW-DFT [e]	1.11
E. Ziambaras et al. 2007 [S7]	vdW-DFT [e]	1.22
S. Lebègue *et al.* 2010 [S8]	ACFDT-RPA [f]	1.11
J. Björk *et al*. 2010 [S9]	vdW-DFT [e]	1.13
A. Ambrosetti *et al.* 2014 [S10]	PBE0+MBD@rsSCS [g]	1.15
This study	**DFT-D3**	**1.19**

[a] Transmission electron microscopy

[b] Temperature programmed desorption spectroscopy

[c] Atomic force microscopy

[d] Scanning Tunneling microscopy

[e] van der Waals density functional calculation

[f] Adiabatic-connection fluctuation-dissipation theorem in the direct random phase approximation

[g] PBE density functional calculation with a self-consistent screening and a many body-dispersion correction

[References]

S1. L. X. Benedict, N. G. Chopra, M. L. Cohen, A. Zettl, S. G. Louie and V. H. Crespi, *Chem. Phys. Lett.*, 1998, **286**, 490-496.

S2. R. Zacharia, H. Ulbricht and T. Hertel, *Phys. Rev*. B, 2004, **69**, 155406.

S3. E. Koren, E. Lörtscher, C. Rawlings, A. W. Knoll and U. Duerig, *Science*, 2015, **348**, 679-683.

S4. J. Wang, D. C. Sorescu, S. Jeon, A. Belianinov, S. V. Kalinin, A. P. Baddorf and P. Maksymovych, *Nat. Commun*., 2016, **7**, 13263.

S5. J. Weippert, J. Hauns, J. Bachmann, A. Böttcher, X. Yao, B. Yang, A. Narita, K. Müllen and M. M. Kappes, *J. Chem. Phys.*, 2018, **149**, 194701.

S6. S. D. Chakarova-Käck, E. Schröder, B. I. Lundqvist and D. C. Langreth, *Phys. Rev*. B, 2006, **96**, 146107.

S7. E. Ziambaras, J. Kleis, E. Schröder and P. Hyldgaard, *Phys. Rev*. B, 2007, **76**, 155425.

S8. S. Lebègue, J. Harl, T. Gould, J. G. Ángyán, G. Kresse and J. F. Dobson, *Phys. Rev. Lett.,* 2010, **105**, 196401.

S9. J. Björk, F. Hanke, C.-A. Palma, P. Samori, M. Cecchini and M. Persson, *J. Phys. Chem. Lett.,* 2010, **1**, 3407-3412.

S10. A. Ambrosetti, A. M. Reilly, R. A. DiStasio, Jr. and A. Tkatchenko, *J. Chem. Phys*., 2014, **140**, 18A508.

4. E_{int} calculated for $C_{96}H_{24}$ complexes with PAHs and mean distances of carbon atoms of PAHs from $C_{96}H_{24}$ plane

Table S2 B3LYP-D3/6-311G** level E_{int} and mean distance of carbon atoms in PAHs from the π-plane of $C_{96}H_{24}$ (R) in optimised geometry.

Adsorbate	Formula	E_{int} / kcal mol^{-1}	R / Å
Benzene	C_6H_6	–10.55	3.39
Naphthalene	$C_{10}H_8$	–16.57	3.39
Anthracene	$C_{14}H_{10}$	–22.62	3.39
Phenanthrene	$C_{14}H_{10}$	–22.70	3.39
Pyrene	$C_{16}H_{10}$	–25.23	3.40
Tetracene	$C_{18}H_{12}$	–28.47	3.39
Triphenylene	$C_{18}H_{12}$	–28.61	3.39
Perylene	$C_{20}H_{12}$	–31.25	3.39
Coronene	$C_{24}H_{12}$	–35.80	3.39
Ovalene	$C_{32}H_{14}$	–46.37	3.40
Circumpyrene	$C_{42}H_{16}$	–58.05	3.41

5. E_{int} and ΔE_{int} calculated using different basis sets

Table S3 B3LYP-D3 level E_{int} and ΔE_{int} calculated for $C_{54}H_{18}$-benzene complex associated with horizontal displacement of benzene along *y*-axis using different basis sets. The plots of ΔE_{int} as a function of displacement are shown in Fig. S3.

Displacement / Å	B3LYP-D3/6-31G*		B3LYP-D3/6-311G*		B3LYP-D3/6-311G**	
	E_{int} [a]	ΔE_{int} [a]	E_{int} [a]	ΔE_{int} [a]	E_{int} [a]	ΔE_{int} [a]
0	-8.88	0.02	-9.89	0.02	-9.84	0.02
0.2	-8.90	0	-9.91	0	-9.86	0
0.4	-8.83	0.07	-9.84	0.07	-9.78	0.08
0.6	-8.67	0.23	-9.68	0.23	-9.62	0.24
0.8	-8.46	0.44	-9.46	0.45	-9.41	0.45
1.0	-8.24	0.66	-9.24	0.67	-9.19	0.67
1.2	-8.08	0.82	-9.07	0.84	-9.02	0.84
1.4	-8.01	0.89	-9.00	0.91	-8.95	0.91
1.6	-8.05	0.85	-9.05	0.86	-9.00	0.86
1.8	-8.20	0.70	-9.20	0.71	-9.15	0.71
2.0	-8.41	0.49	-9.41	0.5	-9.36	0.5
2.2	-8.63	0.27	-9.64	0.27	-9.58	0.28
2.4	-8.80	0.10	-9.81	0.1	-9.76	0.1
2.6	-8.89	0.01	-9.91	0	-9.85	0.01
2.8	-8.89	0.01	-9.90	0.01	-9.85	0.01

[a] Energy in kcal mol^{-1}.

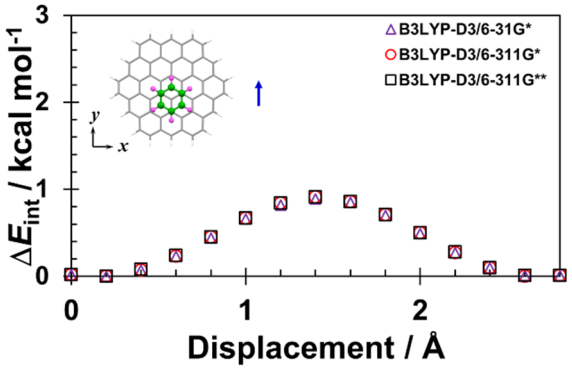

Fig. S3 Plots of B3LYP-D3 level ΔE_{int} calculated for $C_{54}H_{18}$-benzene complex associated with horizontal displacement of benzene along *y*-axis. Purple triangles, red circles and black squares correspond to ΔE_{int} obtained by B3LYP-D3/6-31G*, B3LYP-D3/6-311G*, and B3LYP-D3/6-311G** level calculations, respectively.

6. E_{int} and ΔE_{int} obtained by MP2 and dispersion-corrected double-hybrid DFT calculations

Table S4 E_{int} and ΔE_{int} calculated for $C_{54}H_{18}$-benzene complex associated with horizontal displacement along *y*-axis obtained by MP2 and dispersion-corrected double-hybrid DFT calculations using the 6-311G** basis set. The plots of ΔE_{int} as a function of displacement are shown in Fig. S4.

Displacement / Å	MP2 /6-311G*		B2PLYPD3 /6-311G*		B2PLYPD3-D3 /6-311G*		mPW2PLYPD /6-311G*	
	E_{int} [a]	ΔE_{int} [a]	E_{int} [a]	ΔE_{int} [a]	E_{int} [a]	ΔE_{int} [a]	E_{int} [a]	ΔE_{int} [a]
0	-11.95	0.03	-9.99	0.02	-8.91	0.03	-8.01	0.01
0.2	-11.98	0	-10.01	0	-8.94	0	-8.02	0
0.4	-11.92	0.06	-9.94	0.07	-8.86	0.08	-7.94	0.08
0.6	-11.76	0.22	-9.77	0.24	-8.70	0.24	-7.78	0.24
0.8	-11.54	0.44	-9.55	0.46	-8.47	0.47	-7.55	0.47
1.0	-11.32	0.66	-9.33	0.68	-8.23	0.71	-7.32	0.70
1.2	-11.14	0.84	-9.16	0.85	-8.06	0.88	-7.15	0.87
1.4	-11.07	0.91	-9.08	0.93	-7.98	0.96	-7.07	0.95
1.6	-11.12	0.86	-9.13	0.88	-8.03	0.91	-7.12	0.90
1.8	-11.28	0.70	-9.29	0.72	-8.19	0.75	-7.28	0.74
2.0	-11.50	0.48	-9.51	0.50	-8.42	0.52	-7.51	0.51
2.2	-11.72	0.26	-9.74	0.27	-8.66	0.28	-7.74	0.28
2.4	-11.90	0.08	-9.91	0.10	-8.84	0.10	-7.92	0.10
2.6	-11.98	0	-10.00	0.01	-8.93	0.01	-8.01	0.01
2.8	-11.96	0.02	-10.00	0.01	-8.92	0.02	-8.02	0

[a] Energy in kcal mol^{-1}.

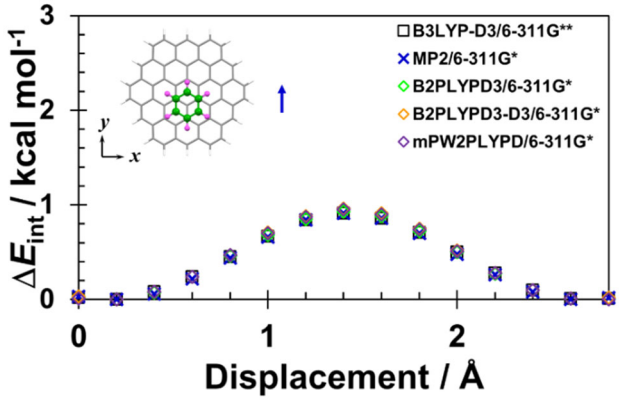

Fig. S4 Plots of ΔE_{int} for $C_{54}H_{18}$-benzene complex associated with associated with horizontal displacements of benzene along *y*-axis on $C_{54}H_{18}$, obtained by B3LYP-D3, MP2 and dispersion-corrected double-hybrid DFT calculations using 6-311G** basis set. Black squares, blue cross marks, light green rhombi, orange rhombi and purple rhombi correspond to ΔE_{int} obtained by B3LYP-D3/6-311G**, MP2/6-311G*, B2PLYPD3/6-311G*, B2PLYPD3-D3/6-311G*, and mPW2PLYPD/6-311G* level calculations, respectively. B2PLYPD3-D3 is B2PLYP calculation with Grimme's D3 correction. B2PLYPD3 is B2PLYP calculation with Grimme's D3BJ correction.

7. BLYP-D3 and PBE-D3 level E_{int} and ΔE_{int}

Table S5 BLYP-D3 and PBE-D3 level E_{int} and ΔE_{int} calculated for $C_{54}H_{18}$-benzene complex associated with horizontal displacement of benzene along *y*-axis using 6-311G** basis set. The plots of ΔE_{int} as a function of displacement are shown in Fig. S5.

Displacement / Å	BLYP-D3/6-311G**		PBE-D3/6-311G**	
	E_{int} [a]	ΔE_{int} [a]	E_{int} [a]	ΔE_{int} [a]
0	-10.48	0.02	-9.06	0.01
0.2	-10.50	0	-9.07	0
0.4	-10.43	0.07	-9.00	0.07
0.6	-10.28	0.22	-8.84	0.23
0.8	-10.08	0.42	-8.63	0.44
1.0	-9.87	0.63	-8.42	0.65
1.2	-9.71	0.79	-8.25	0.82
1.4	-9.64	0.86	-8.19	0.88
1.6	-9.69	0.81	-8.23	0.84
1.8	-9.83	0.67	-8.38	0.69
2.0	-10.04	0.46	-8.59	0.48
2.2	-10.25	0.25	-8.80	0.27
2.4	-10.41	0.09	-8.97	0.10
2.6	-10.49	0.01	-9.06	0.01
2.8	-10.49	0.01	-9.07	0

[a] Energy in kcal mol^{-1}.

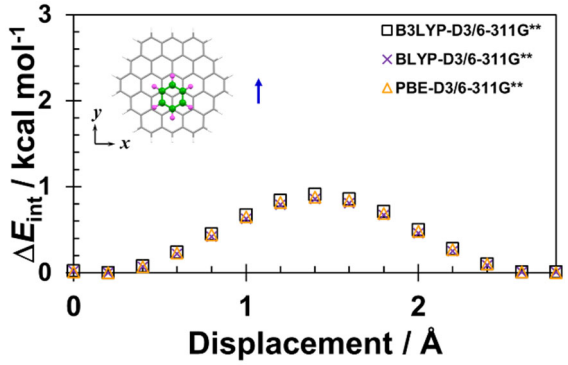

Fig. S5 Plots of BLYP-D3 and PBE-D3 level ΔE_{int} calculated for $C_{54}H_{18}$-benzene complex associated with horizontal displacement of benzene along *y*-axis using the 6-311G** basis set. Black squares, purple cross marks and orange triangles correspond to ΔE_{int} obtained by B3LYP-D3/6-311G**, BLYP-D3/6-311G**, and PBE-D3/6-311G** level calculations, respectively.

8. E_{int} and ΔE_{int} calculated for $C_{96}H_{24}$-benzene complex associated with horizontal displacement

Table S6 B3LYP-D3/6-311G** level E_{int} and ΔE_{int} calculated for $C_{96}H_{24}$-benzene complex with horizontal displacement of benzene along the directions those make angles of 0˚, 30˚, 60˚ and 90˚ with the *x*-axis, respectively. $E_{int(max)}$ values (maximum values of E_{int}) are coloured in red. The plots of ΔE_{int} as a function of displacement are shown in Figs. 3 and 4.

Displacement / Å	0˚ (*x*-axis)		30˚		60˚		90˚ (*y*-axis)	
	E_{int} [a]	ΔE_{int} [a]	E_{int} [a]	ΔE_{int} [a]	E_{int} [a]	ΔE_{int} [a]	E_{int} [a]	ΔE_{int} [a]
0	-10.43	0	-10.43	0	-10.43	0	-10.43	0
0.2	-10.40	0.03	-10.40	0.03	-10.40	0.03	-10.40	0.03
0.4	-10.31	0.12	-10.36	0.07	-10.33	0.1	-10.30	0.13
0.6	-10.19	0.24	-10.32	0.11	-10.23	0.2	-10.13	0.30
0.8	-10.07	0.36	-10.31	0.12	-10.13	0.3	-9.92	0.51
1.0	-9.98	0.45	-10.35	0.08	-10.05	0.38	-9.72	0.71
1.2	-9.94	0.49	-10.40	0.03	-10.02	0.41	-9.56	0.87
1.4	-9.96	0.47	-10.43	0	-10.04	0.39	-9.50	0.93
1.6	-10.02	0.41			-10.10	0.33	-9.54	0.89
1.8	-10.11	0.32			-10.19	0.24	-9.67	0.76
2.0	-10.21	0.22			-10.30	0.13	-9.87	0.56
2.2	-10.28	0.15			-10.38	0.05	-10.09	0.34
2.4	-10.29	0.14			-10.43	0	-10.27	0.16
2.6							-10.38	0.05
2.8							-10.43	0

[a] Energy in kcal mol^{-1}.

9. Comparison of HF and MP2 level ΔE_{int}

Table S7 HF level E_{int} and ΔE_{int} calculated for $C_{54}H_{18}$-benzene complex associated with horizontal displacement of benzene along *y*-axis. The plots of ΔE_{int} as a function of displacement are shown in Fig. S6.

Displacement / Å	HF/6-311G*	
	E_{int} [a]	ΔE_{int} [a]
0	5.69	0.01
0.2	5.70	0.02
0.4	5.84	0.16
0.6	6.10	0.42
0.8	6.43	0.75
1.0	6.76	1.08
1.2	7.01	1.33
1.4	7.12	1.44
1.6	7.04	1.36
1.8	6.82	1.14
2.0	6.49	0.81
2.2	6.16	0.48
2.4	5.88	0.20
2.6	5.72	0.04
2.8	5.68	0

[a] Energy in kcal mol^{-1}.

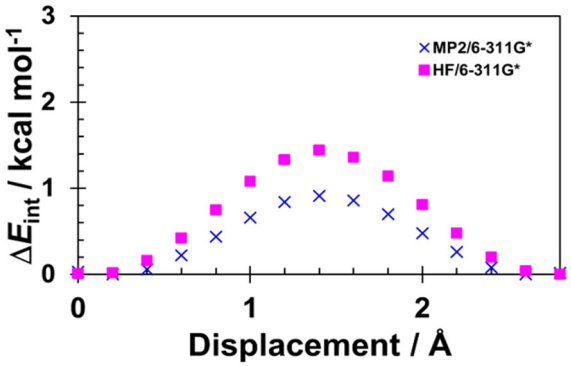

Fig. S6 Plots of HF and MP2 level ΔE_{int} calculated for $C_{54}H_{18}$-benzene complex associated with horizontal displacement of benzene along *y*-axis using the 6-311G* basis set. Blue cross marks and pink squares correspond to ΔE_{int} obtained by MP2/6-311G* and HF/6-311G* level calculations, respectively.

10. E_{int} and ΔE_{int} calculated for $C_{96}H_{24}$-benzene complexes with naphthalene and anthracene associated with horizontal displacement

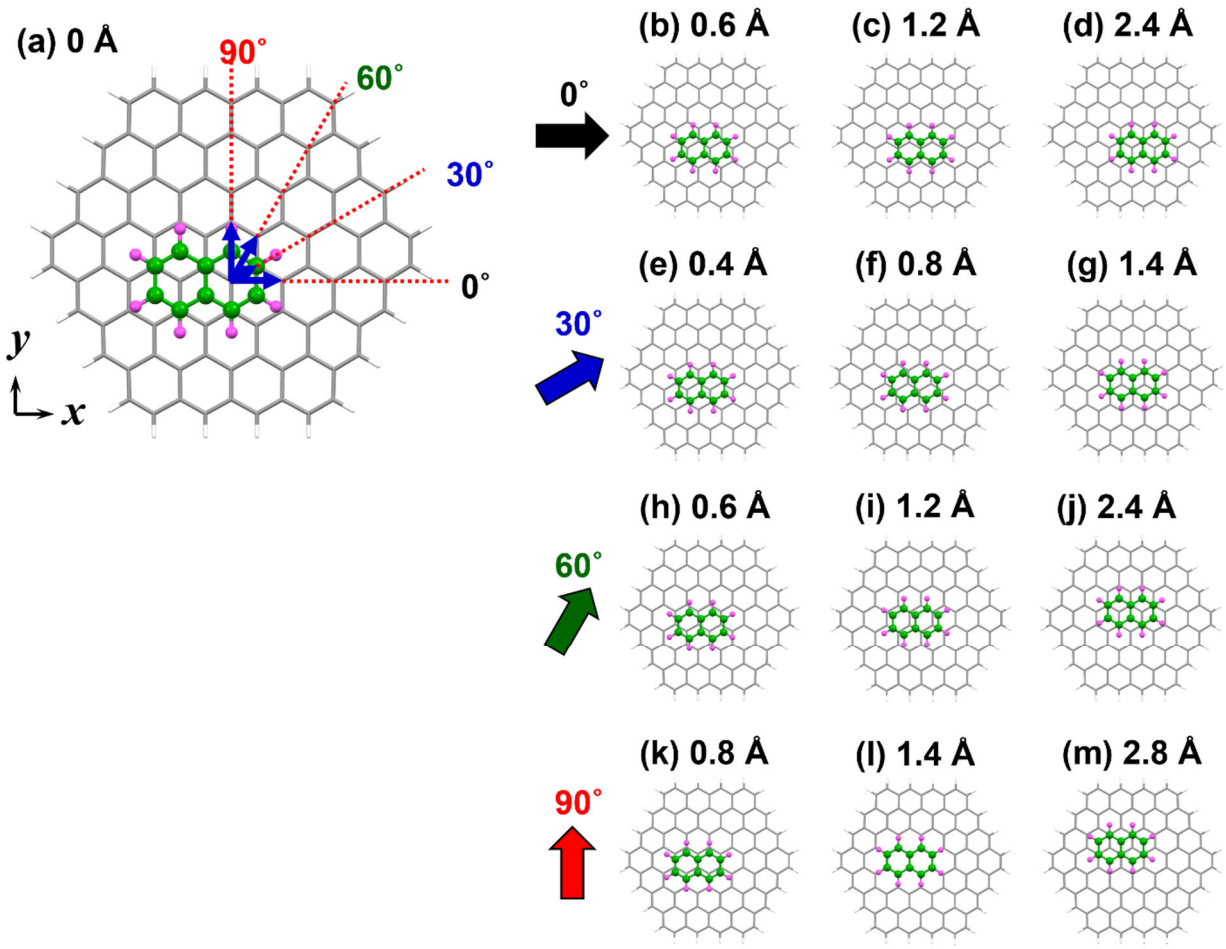

Fig. S7 Horizontal displacement of naphthalene in $C_{96}H_{24}$-naphthalene complex: (a) The AB-stacking structure (initial position) of the complex and the directions of displacement of naphthalene; naphthalene was moved horizontally along the directions that resulted in angles of 0˚ (b-d), 30˚ (e-g), 60˚ (h-j), 90˚ (k-m) with the *x*-axis.

Table S8 B3LYP-D3/6-311G** level E_{int} and ΔE_{int} calculated for $C_{96}H_{24}$-naphthalene complex with horizontal displacement of naphthalene along the directions that resulted in angles of 0˚, 30˚, 60˚ and 90˚ with the *x*-axis, respectively. The plots of ΔE_{int} as a function of displacement are shown in Fig. 4. $E_{int(max)}$ values (maximum values of E_{int}) are coloured in red.

Displacement / Å	0˚ (*x*-axis)		30˚		60˚		90˚ (*y*-axis)	
	E_{int} [a]	ΔE_{int} [a]	E_{int} [a]	ΔE_{int} [a]	E_{int} [a]	ΔE_{int} [a]	E_{int} [a]	ΔE_{int} [a]
0	-16.36	0	-16.36	0.12	-16.37	0.11	-16.36	0.01
0.2	-16.34	0.02	-16.37	0.11	-16.34	0.14	-16.34	0.03
0.4	-16.22	0.14	-16.32	0.16	-16.23	0.25	-16.19	0.18
0.6	-16.05	0.31	-16.29	0.19	-16.06	0.42	-15.90	0.47
0.8	-15.87	0.49	-16.30	0.18	-15.89	0.59	-15.53	0.84
1.0	-15.74	0.62	-16.36	0.12	-15.75	0.73	-15.16	1.21
1.2	-15.68	0.68	-16.44	0.04	-15.70	0.78	-14.89	1.48
1.4	-15.71	0.65	-16.48	0	-15.73	0.75	-14.77	1.60
1.6	-15.83	0.53			-15.85	0.63	-14.84	1.53
1.8	-16.00	0.36			-16.04	0.44	-15.09	1.28
2.0	-16.17	0.19			-16.24	0.24	-15.45	0.92
2.2	-16.31	0.05			-16.40	0.08	-15.83	0.54
2.4	-16.36	0			-16.48	0	-16.13	0.24
2.6							-16.32	0.05
2.8							-16.37	0

[a] Energy in kcal mol^{-1}.

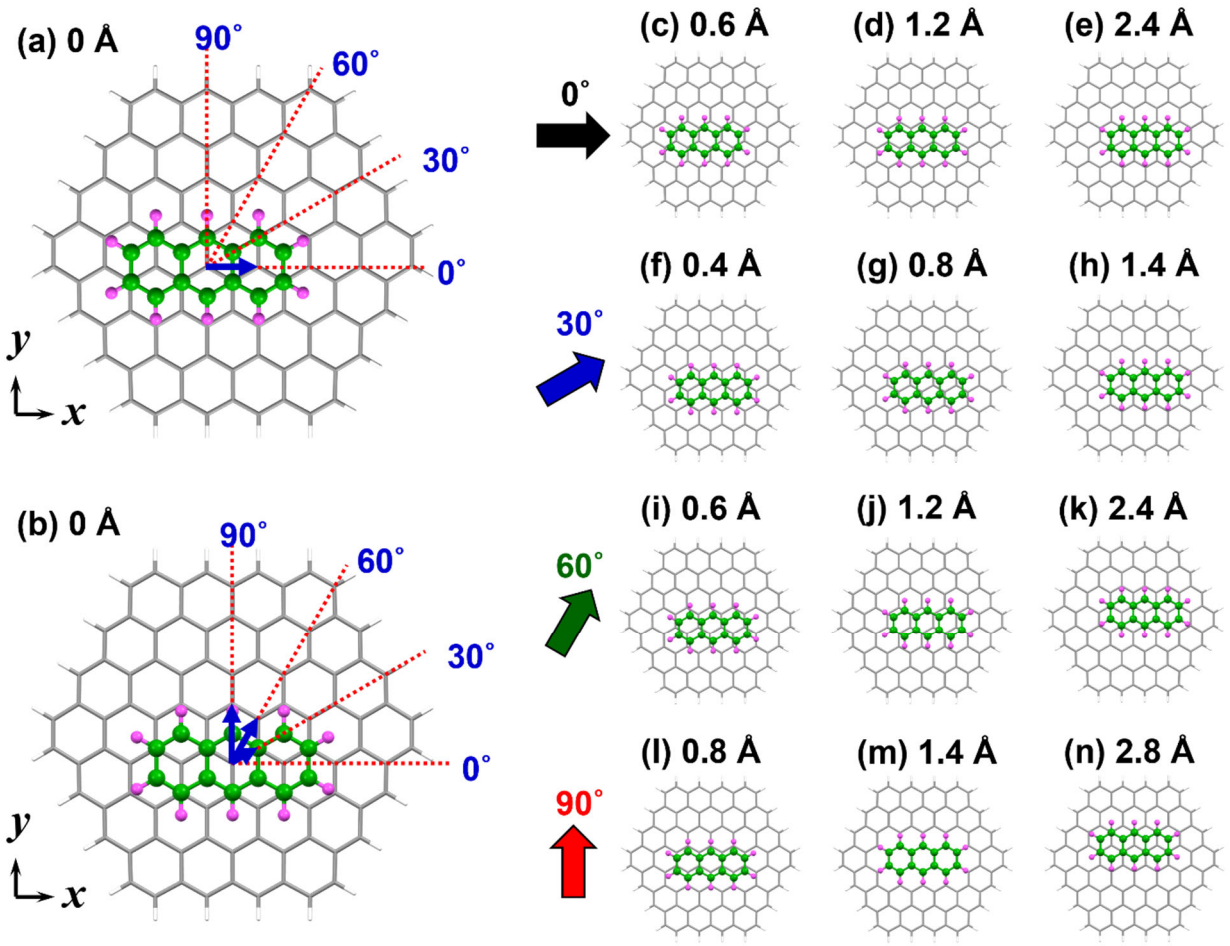

Fig. S8 Horizontal displacement of anthracene in $C_{96}H_{24}$-anthracene complexes; (a, b) The AB-stacking structure (initial position) of the complexes and the directions of displacement of anthracene; anthracene was moved horizontally along the directions that resulted in angles of 0˚ (c-e), 30˚ (f-h), 60˚ (i-k), 90˚ (l-n) with the *x*-axis.

Table S9 B3LYP-D3/6-311G** level E_{int} and ΔE_{int} calculated for $C_{96}H_{24}$-anthracene complex with horizontal displacement of anthracene along the directions that resulted in angles of 0˚, 30˚, 60˚ and 90˚ with the *x*-axis, respectively. $E_{int(max)}$ values (maximum values of E_{int}) are coloured in red. The plots of ΔE_{int} as a function of displacement are shown in Fig. 4.

Displacement / Å	0˚ (*x*-axis)		30˚		60˚		90˚ (*y*-axis)	
	E_{int} [a]	ΔE_{int} [a]	E_{int} [a]	ΔE_{int} [a]	E_{int} [a]	ΔE_{int} [a]	E_{int} [a]	ΔE_{int} [a]
0	-22.27	0.01	-22.34	0	-22.34	0	-22.34	0
0.2	-22.25	0.03	-22.29	0.05	-22.27	0.07	-22.31	0.03
0.4	-22.11	0.17	-22.18	0.16	-22.09	0.25	-22.10	0.24
0.6	-21.90	0.38	-22.10	0.24	-21.85	0.49	-21.71	0.63
0.8	-21.68	0.60	-22.10	0.24	-21.61	0.73	-21.22	1.12
1.0	-21.52	0.76	-22.17	0.17	-21.44	0.90	-20.73	1.61
1.2	-21.45	0.83	-22.25	0.09	-21.38	0.96	-20.36	1.98
1.4	-21.48	0.80	-22.27	0.07	-21.43	0.91	-20.20	2.14
1.6	-21.62	0.66			-21.59	0.75	-20.30	2.04
1.8	-21.82	0.46			-21.82	0.52	-20.63	1.71
2.0	-22.04	0.24			-22.05	0.29	-21.10	1.24
2.2	-22.21	0.07			-22.22	0.12	-21.60	0.74
2.4	-22.28	0			-22.27	0.07	-22.02	0.32
2.6							-22.28	0.06
2.8							-22.34	0

[a] Energy in kcal mol^{-1}.

11. Effect of molecular shape on $\Delta E_{int(max)}$ associated with displacement in the 90° direction

The $\Delta E_{int(max)}$ values associated with displacement in the 90° direction were plotted as a function of N_c (Fig. S9). The $\Delta E_{int(max)}$ and $\Delta E_{int(max)}$ per Nc of linear PAHs (benzene, naphthalene, anthracene and tetracene) was compared with that of non-linear shaped PAHs (phenanthrene, pyrene, triphenylene, perylene and coronene). Even when the molecular shape of PAHs was different but N_c was the same (e.g., anthracene and phenanthrene; tetracene and triphenylene), the $\Delta E_{int(max)}$ values showed no significant difference. Individual $\Delta E_{int(max)}$ plots of linear and non-linear shaped PAHs revealed that the $\Delta E_{int(max)}$ per N_c was almost same (0.20 kcal mol^{-1}), suggesting that the shape of the PAHs has little effect on the linear increase in $\Delta E_{int(max)}$ with N_c.

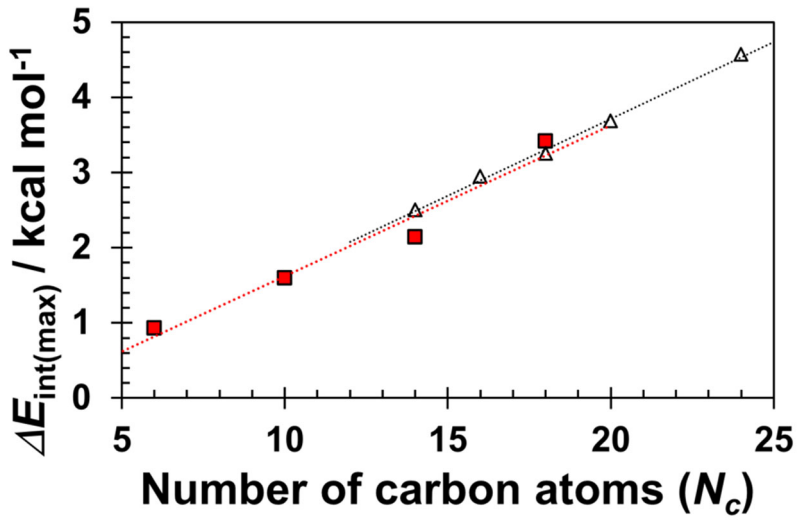

Fig. S9 Plots of $\Delta E_{int(max)}$ associated with displacement in the 90° direction as a function of N_c at the B3LYP-D3/6-311G**: Red circles are plots of linear PAHs (benzene, naphthalene, anthracene and tetracene), and the linear regression equation (red dotted line) is $\Delta E_{int(max)} = 0.20N_c - 0.38$ ($R^2 = 0.961$); black triangles are plots of non-linear shaped PAHs (phenanthrene, pyrene, triphenylene, perylene and coronene), and the linear regression equation (black dotted line) is $\Delta E_{int(max)} = 0.20N_c - 0.37$ ($R^2 = 0.997$): kcal mol^{-1}.

12. ΔE_{int} change associated with the rotation of PAHs

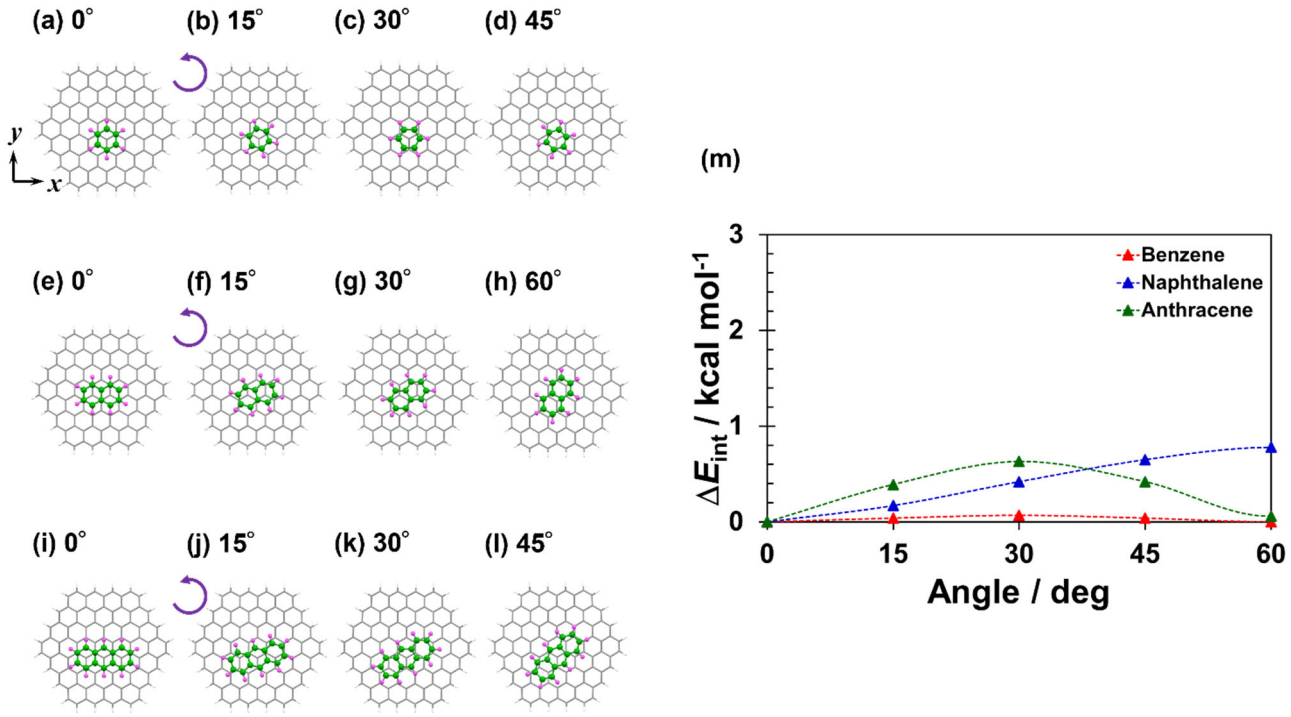

Fig. S10 Rotation of (a-d) benzene, (e-h) naphthalene, (i-l) anthracene in their complexes with $C_{96}H_{24}$, and (m) plots of ΔE_{int} associated with the rotation: Red, blue and green triangles indicate ΔE_{int} calculated for benzene, naphthalene and anthracene complexes, respectively.

Table S10 B3LYP-D3/6-311G** level E_{int} and ΔE_{int} calculated for $C_{96}H_{24}$-PAHs complexes associated with the rotation. The plots of ΔE_{int} as a function of the rotation are shown in Fig. S9.

Angle/ degree	Benzene		Naphthalene		Anthracene	
	E_{int} [a]	ΔE_{int} [a]	E_{int} [a]	ΔE_{int} [a]	E_{int} [a]	ΔE_{int} [a]
0	-10.43	0	-16.48	0	-22.34	0
15	-10.39	0.04	-16.31	0.17	-21.94	0.40
30	-10.36	0.07	-16.06	0.42	-21.71	0.63
45	-10.39	0.04	-15.83	0.65	-21.92	0.42
60	-10.43	0	-15.70	0.78	-22.27	0.07

[a] Energy in kcal mol^{-1}.

13. Comparison of E_{int} calculated for $C_{96}H_{24}$ complexes with PAHs and *n*-alkanes

Geometries of *n*-alkanes on $C_{96}H_{24}$ were optimised by B3LYP-D3/6-31G* level calculations, and each E_{int} value was obtained by B3LYP-D3/6-311G** level calculations. BSSE was corrected using the counterpoise method. The E_{int} is listed in Table S11. The $|E_{int}|$ of *n*-alkanes are plotted as a function of the number of carbon atoms (N_c), and compared with those of PAHs, as shown in Fig. S11.

Table S11 B3LYP-D3/6-311G level E_{int} and mean distance of carbon atoms in *n*-alkanes from the π-plane of $C_{96}H_{24}$ (*R*) in optimised geometry.**

Adsorbate	Formula	E_{int} / kcal mol^{-1}	*R* / Å
methane	CH_4	-3.33	3.36
ethane	C_2H_6	-5.30	3.48
propane	C_3H_8	-7.43	3.49
n-butane	C_4H_{10}	-9.57	3.50
n-pentane	C_5H_{12}	-11.72	3.50
n-hexane	C_6H_{14}	-13.81	3.51
n-heptane	C_7H_{16}	-15.89	3.51
n-octane	C_8H_{18}	-17.91	3.51
n-nonane	C_9H_{20}	-19.92	3.52
n-decane	$C_{10}H_{22}$	-21.72	3.52
n-undecane	$C_{11}H_{24}$	-23.49	3.53
n-dodecane	$C_{12}H_{26}$	-24.89	3.54
n-tridecane	$C_{13}H_{28}$	-26.26	3.55

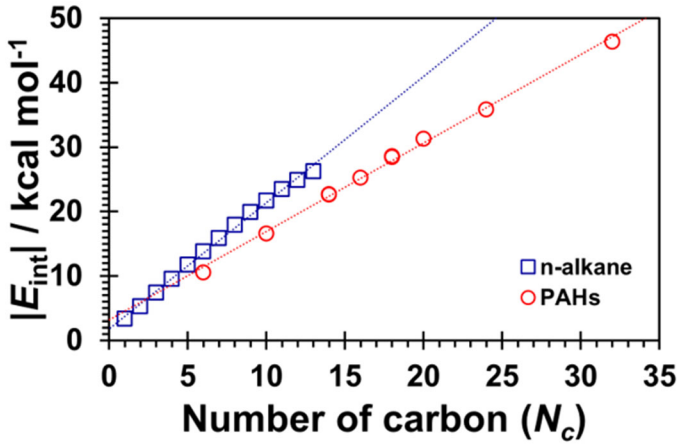

Fig. S11 Plots of $|E_{int}|$ as a function of the number of carbon atoms in n-alkane and PAH (N_c): Red circles are plots of $|E_{int}|$ for $C_{96}H_{24}$ complexes with PAHs obtained at the B3LYP-D3/6-311G** level (Table S1), and their linear fitting (red dotted line) is $|E_{int}| = 1.31N_c + 4.14$ ($R^2 = 0.997$); Blue rhombi are plots of $|E_{int}|$ for for $C_{96}H_{24}$ complexes with *n*-alkanes obtained at the B3LYP-D3/6-311G** level (Table S11), and their linear fitting (blue dotted line) is $|E_{int}| = 1.96N_c + 1.76$ ($R^2 = 0.997$).

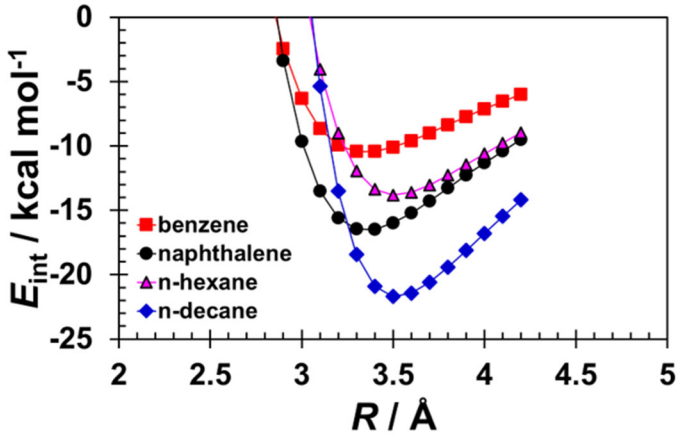

Fig. S12 Interaction energies (E_{int}) calculated for $C_{96}H_{24}$ complexes with benzene, naphthalene, *n*-hexane and *n*-decane with changing distances (R) from π plane of $C_{96}H_{24}$ in optimized geometries of stable structures: red square, black circle, pink triangle and blue rhombi correspond to E_{int} of benzene, naphthalene, *n*-hexane and *n*-decane complexes, respectively.